

# Improved limits on $\bar{\nu}_e$ emission from $\mu^+$ decay

B. Armbruster<sup>a</sup>, G. Drexlin<sup>a</sup>, K. Eitel<sup>a</sup>, T. Jannakos<sup>a</sup>, J. Kleinfeller<sup>a</sup>, R. Maschuwa<sup>a,c</sup>,  
C. Oehler<sup>a</sup>, P. Plischke<sup>a</sup>, J. Reichenbacher<sup>a</sup>, M. Steidl<sup>a</sup>, B. Zeitnitz<sup>a,e</sup>, H. Gemmeke<sup>b</sup>,  
M. Kleifges<sup>b</sup>, C. Eichner<sup>c</sup>, C. Ruf<sup>c</sup>, B.A. Bodmann<sup>d</sup>, E. Finckh<sup>d</sup>, J. Höbl<sup>d</sup>,  
P. Jünger<sup>d</sup>, W. Kretschmer<sup>d</sup>, J. Wolfe<sup>e</sup>, N.E. Booth<sup>f</sup>, I.M. Blair<sup>g</sup>, J.A. Edgington<sup>g</sup>

<sup>a</sup> *Institut für Kernphysik, Forschungszentrum Karlsruhe, 76021 Karlsruhe, Germany*

<sup>b</sup> *Institut für Prozessdatenverarbeitung und Elektronik,*

*Forschungszentrum Karlsruhe, 76021 Karlsruhe, Germany*

<sup>c</sup> *Institut für Strahlen- und Kernphysik, Universität Bonn, Nußallee 14-16, 53115 Bonn, Germany*

<sup>d</sup> *Physikalisches Institut, Universität Erlangen-Nürnberg, Erwin-Rommel-Str. 1, 91058 Erlangen, Germany*

<sup>e</sup> *Institut für experimentelle Kernphysik, Universität Karlsruhe, Gaede-Str. 1, 76128 Karlsruhe, Germany*

<sup>f</sup> *Department of Physics, University of Oxford, Keble Road, Oxford OX1 3RH, United Kingdom*

<sup>g</sup> *Physics Department, Queen Mary, University London, Mile End Road, London E1 4NS, United Kingdom*

(Dated: February 14, 2003)

## Abstract

We investigated  $\mu^+$  decays at rest produced at the ISIS beam stop target. Lepton flavor (LF) conservation has been tested by searching for  $\bar{\nu}_e$  via the detection reaction  $p(\bar{\nu}_e, e^+)n$ . No  $\bar{\nu}_e$  signal from LF violating  $\mu^+$  decays was identified. We extract upper limits of the branching ratio for the LF violating decay  $\mu^+ \rightarrow e^+ + \bar{\nu}_e + (\bar{\nu})$  compared to the Standard Model (SM)  $\mu^+ \rightarrow e^+ + \nu_e + \bar{\nu}_\mu$  decay:  $BR < 0.9(1.7) \cdot 10^{-3}$  (90% C.L.) depending on the spectral distribution of  $\bar{\nu}_e$  characterized by the Michel parameter  $\tilde{\rho} = 0.75(0.0)$ . These results improve earlier limits by one order of magnitude and restrict extensions of the SM in which  $\bar{\nu}_e$  emission from  $\mu^+$  decay is allowed with considerable strength. The decay  $\mu^+ \rightarrow e^+ + \bar{\nu}_e + \nu_\mu$  as source for the  $\bar{\nu}_e$  signal observed in the LSND experiment can be excluded.

PACS numbers: 13.35.Bv, 14.60.St, 11.30.Fs

## INTRODUCTION

In the Standard Model (SM), the main decay mode of positive muons is the decay into a positron and two neutrinos  $\mu^+ \rightarrow e^+ + \nu + \nu'$ . Assuming conservation of the additive lepton family or flavor (LF) numbers  $L_e$  and  $L_\mu$ , the neutrino flavors are fixed to be  $\nu = \nu_e$  and  $\nu' = \bar{\nu}_\mu$ . The neutrinos are massless with the  $\nu_e$  being a left-handed neutrino, the  $\bar{\nu}_\mu$  a right-handed anti-neutrino. The structure of the muon decay can be described by the V–A theory of weak interactions. Therefore  $\mu$  decay as a purely leptonic process has been used to study with high precision the SM of weak interactions. The Lorentzian V–A structure of the  $\mu^+$  decay can be tested by measuring the massive leptons, i.e. the initial  $\mu^+$  and the final  $e^+$  [1] or by investigating the neutrino energy spectrum [2]. However, to test conservation of the LF numbers  $L_e$  and  $L_\mu$  in  $\mu$  decay it is essential to observe the final neutrino states [3]. All tests so far show no deviations from the SM.

However, the LF number violating decay mode  $\mu^+ \rightarrow e^+ + \bar{\nu}_e + \nu_\mu$  is allowed in many extensions of the SM, e.g. left–right (LR) symmetric models [4, 5, 6, 7], GUT models with dileptonic gauge bosons [8], extensions involving additional scalar multiplets [9] or supersymmetric models with R parity violation [10], together with the LF number violating decay  $\mu^+ \rightarrow e^+ + \gamma$  [11]. Although the energy scale of LR symmetry of weak interactions or the appearance of supersymmetric particles is expected to be in the range of 0.1–1 TeV, precision measurements at intermediate energies can provide essential restraints on the parameters used in various models. Therefore, the detailed investigation of the  $\mu^+$  decay plays a major role in determining the structure of weak interactions and the precision of lepton number conservation.

On the other hand, there are clear evidences for neutrino oscillations from experiments on atmospheric, solar and reactor neutrinos [13]. Since  $\nu$  oscillations violate the conservation of the lepton family numbers, such results enhance the interest of searching for direct LF number violation. In addition, there is a positive  $\bar{\nu}_e$  signal from the accelerator experiment LSND [14] which could be explained a priori as an indication for  $\bar{\nu}_\mu \rightarrow \bar{\nu}_e$  oscillations of  $\bar{\nu}_\mu$  from  $\mu^+ \rightarrow e^+ + \nu_e + \bar{\nu}_\mu$  or directly for the decay mode  $\mu^+ \rightarrow e^+ + \bar{\nu}_e + (\bar{\nu})$ . Due to limited statistics and energy resolution, this ambiguity is not resolved by the LSND experiment itself.

The spallation source ISIS at the Rutherford Laboratory, UK, is a unique source of  $\mu^+$

to study such decays. The **K**arlsruhe **R**utherford **M**edium **E**nergy **N**eutrino experiment investigated the neutrinos produced at ISIS through the decays of  $\pi^+$  and  $\mu^+$  at rest. One purpose of the KARMEN experiment was the investigation of  $\nu$ -nucleus interactions on  $^{12}\text{C}$  [15]. The good agreement of the measurements with theoretical predictions allowed a sensitive search for processes forbidden in the SM such as  $\nu$ -oscillations,  $\nu_\mu \rightarrow \nu_e$  and  $\bar{\nu}_\mu \rightarrow \bar{\nu}_e$  in the appearance mode [16] and  $\nu_e \rightarrow \nu_x$  in the disappearance mode [17] or non-SM decay modes of  $\pi^+$  and  $\mu^+$ .

In this letter we report the results of the search for  $\bar{\nu}_e$  from  $\mu^+$  decay at rest (DAR). Note that  $\bar{\nu}_e$  from non SM interactions can be produced by either  $\mu^+ \rightarrow e^+ + \bar{\nu}_e + (\bar{\nu})$  in the ISIS target or by oscillations  $\bar{\nu}_\mu \rightarrow \bar{\nu}_e$  of  $\bar{\nu}_\mu$  on their way to the detector with  $\bar{\nu}_\mu$  being produced at ISIS in SM  $\mu^+$  decays. While the  $\bar{\nu}_e$  energy spectrum is fixed in the DAR  $\mu^+ \rightarrow e^+ + \bar{\nu}_e + (\bar{\nu})$  with a spatial flux according to a  $r^{-2}$  dependence, the energy and spatial distributions of  $\bar{\nu}_e$  from oscillations strongly depend on the oscillation parameters, i.e. the mass difference  $\Delta m_{ij}^2 = |m_i^2 - m_j^2|$ . With its excellent energy resolution of  $\sigma_E/E = 11\%/\sqrt{E[\text{MeV}]}$ , the KARMEN detector is able to separate different scenarios for potential  $\bar{\nu}_e$  occurrence. Although the search for oscillations  $\bar{\nu}_\mu \rightarrow \bar{\nu}_e$  and for the decay  $\mu^+ \rightarrow e^+ + \bar{\nu}_e + (\bar{\nu})$  use the same detection reaction  $p(\bar{\nu}_e, e^+)n$  for  $\bar{\nu}_e$ , the different physics and consequently the different  $e^+$  spectral distributions result in two separate analyses.

## $\bar{\nu}_e$ FROM LF VIOLATING $\mu^+$ DECAYS

In the SM, applying the V-A theory, the energy spectra of massless neutrinos from  $\mu^+$  decay  $\mu^+ \rightarrow e^+ + \nu_e + \bar{\nu}_\mu$  can be calculated neglecting radiative corrections as [19]

$$N(\epsilon)d\epsilon \propto \epsilon^2 [3(1 - \epsilon) + \frac{2}{3}\rho(4\epsilon - 3)]d\epsilon \quad (1)$$

with the relative energy  $\epsilon = E_\nu/E_{\text{max}}$ ,  $E_{\text{max}} = 52.83 \text{ MeV}$  for the decay at rest, and the Michel parameter  $\rho = 0(0.75)$  for  $\nu_e(\bar{\nu}_\mu)$ , respectively.

Looking for physics beyond the SM,  $\bar{\nu}_e$ 's from  $\mu^+ \rightarrow e^+ + \bar{\nu}_e + (\bar{\nu})$  in general have non-zero mass and contributions of left- or right-handed chirality eigenstates. As only the  $\bar{\nu}_e$  in the decay  $\mu^+ \rightarrow e^+ + \bar{\nu}_e + (\bar{\nu})$  is identified in the experiment, the second emitted (anti)neutrino  $(\bar{\nu})$  is not determined. Since our experimental result sets upper limits on  $\mu^+ \rightarrow e^+ + \bar{\nu}_e + (\bar{\nu})$ , these limits also apply for the specific case  $(\bar{\nu}) = \nu_\mu$ , which is the

dominant one for certain model assumptions [? ].

Taking the actual direct mass limits for  $\bar{\nu}_e$ ,  $m(\bar{\nu}_e) < 2.2 \text{ eV}$  [18] (and hence for  $\nu_\mu$  and  $\nu_\tau$  masses through the mixing manifested in the experiments on neutrino oscillations), the  $\nu$  masses are very small compared to the mass of the charged leptons or the energy scale of the neutrinos from  $\mu^+$  decays at rest. Assuming Majorana type neutrinos, the  $\nu_e$  of left-handed chirality emitted in the SM decay  $\mu^+ \rightarrow e^+ + \nu_e + \bar{\nu}_\mu$  could be detected via the reaction  $p(\bar{\nu}_e, e^+)n$  since there is no distinction between  $\nu_e$  and  $\bar{\nu}_e$ . However, the detection of  $\bar{\nu}_e$ 's emitted in muon decays with left-handed helicity would be strongly helicity-suppressed ( $1-\beta \approx o(10^{-14})$  for a neutrino of 10 MeV energy and a rest mass of  $2 \text{ eV}/c^2$ ) since only right-handed anti-neutrinos are absorbed via  $p(\bar{\nu}_e, e^+)n$ . In the case of Dirac type neutrinos, the above argument applies for left-handed chirality states of the  $\bar{\nu}_e$  emitted. Therefore, KARMEN as any detector up to date is sensitive only to right-handed  $\bar{\nu}_e$ 's.

With the rest masses much smaller than the energy of all neutrinos emitted in  $\mu^+ \rightarrow e^+ + \bar{\nu}_e + (\bar{\nu})$ , an analytical description of the neutrino spectra similar to the one in equ. (1) can be applied, with the spectral parameter  $\tilde{\rho}$  to be specified, replacing the SM Michel parameter  $\rho$ . In some SM extensions with  $\mu^+ \rightarrow e^+ + \bar{\nu}_e + \nu_\mu$ , the  $\bar{\nu}_e$  and  $\nu_\mu$  take the places of the SM  $\bar{\nu}_\mu$  and  $\nu_e$ , respectively, with  $\tilde{\rho}(\bar{\nu}_e) = 0.75$  [5]. In others,  $\tilde{\rho} = 0$  for the emitted  $\bar{\nu}_e$  [9]. In our analysis, we therefore investigate the  $\bar{\nu}_e$  emission for a variety of  $\tilde{\rho}$  parameters.

## EXPERIMENTAL CONFIGURATION AND DATA EVALUATION

The experiment was performed at the neutrino source of the ISIS synchrotron which accelerates protons to an energy of 800 MeV before striking a massive beam stop target. On average,  $4.59 \cdot 10^{-2} \pi^+$  per incident proton are produced which are stopped within the target and decay at rest. Neutrinos emerge isotropically from the consecutive decays at rest (DAR)  $\pi^+ \rightarrow \mu^+ + \nu_\mu$  and  $\mu^+ \rightarrow e^+ + \nu_e + \bar{\nu}_\mu$  [20] assuming the  $\nu$ -flavors of the SM decay channels. Neutrinos from  $\mu^+$  DAR have a continuous energy spectrum according to equ. (1). Due to the narrow time structure of 525 ns of the proton pulses muons are produced in a short time window compared to their lifetime of  $2.2 \mu\text{s}$ .

The neutrinos are detected in a 56 t scintillation calorimeter [21] at a mean distance of 17.6 m from the ISIS target. The calorimeter is a mineral oil based scintillator segmented

into 512 independent modules. Gadolinium within the module walls allows effective neutron detection via  $\text{Gd}(n, \gamma)$  in addition to the capture on the hydrogen of the scintillator via  $\text{p}(n, \gamma)$ . The scintillation detector provides an almost pure target of  $^{12}\text{C}$  and  $^1\text{H}$  for  $\nu$ -interactions. Three veto layers ensure a search for LF violating  $\mu^+$  decays almost free of cosmic background.

$\bar{\nu}_e$ 's from  $\mu^+$  decay can be detected via the  $(e^+, n)$  sequence from charged current reactions  $\text{p}(\bar{\nu}_e, e^+)n$  and  $^{12}\text{C}(\bar{\nu}_e, e^+)n$   $^{11}\text{B}$ . Hence, the signature is a prompt  $e^+$  and a delayed, spatially correlated  $\gamma$  signal from the capture of the thermalized neutron by  $\text{p}(n, \gamma)$  with  $E_\gamma = 2.2\text{ MeV}$  or  $\text{Gd}(n, \gamma)$  with  $\sum E_\gamma = 8\text{ MeV}$ . The flux averaged (taking equ. (1) with  $\rho = 0.75$ ) cross section of  $\text{p}(\bar{\nu}_e, e^+)n$  is  $\sigma = 93.5 \cdot 10^{-42}\text{ cm}^2$  [22]. The  $^{12}\text{C}(\bar{\nu}_e, e^+)n$   $^{11}\text{B}$  contribution to  $(e^+, n)$  sequences has a cross section of  $\sigma = 8.52 \cdot 10^{-42}\text{ cm}^2$  [23] which is further reduced relative to  $\text{p}(\bar{\nu}_e, e^+)n$  by the abundance ratio  $\text{H/C}=1.767$  within the scintillator.

A positron candidate is accepted only if there is no activity in the central detector or in the veto system up to  $24\mu\text{s}$  beforehand. The prompt event is searched for in an interval of  $0.6\mu\text{s}$  to  $10.6\mu\text{s}$  after beam-on-target. The time structure of the prompt  $e^+$  event relative to the proton pulses has to follow the  $\mu^+$  decay time constant of  $2.2\mu\text{s}$ . The expected visible  $e^+$  energy has been simulated in detail based on  $\bar{\nu}_e$  spectra with different values of the parameter  $\tilde{\rho}$  including both detection reactions  $\text{p}(\bar{\nu}_e, e^+)n$  and  $^{12}\text{C}(\bar{\nu}_e, e^+)n$   $^{11}\text{B}$ . As a result, the prompt energy is required to be within  $16\text{ MeV} \leq E(\text{prompt}) \leq 50\text{ MeV}$  (see Fig. 1).

The time difference between the  $e^+$  and the capture  $\gamma$  is given by the thermalization and capture of neutrons and can be approximated by an exponential with a time constant of  $\tau_n \approx 120\mu\text{s}$ . Therefore, the delayed event has to appear within  $1.3\text{ m}^3$  around the prompt event position, correlated in time ( $5\mu\text{s} \leq \Delta t \leq 300\mu\text{s}$ ) with a visible energy  $E(\text{delayed}) \leq 8\text{ MeV}$ . For further details of the data reduction of sequential event signatures and of the neutron detection in KARMEN see also [16].

The raw data investigated in this search were recorded in the measuring period of February 1997 to March 2001 and represent the entire KARMEN 2 data set which corresponds to 9425 C protons on target with  $2.7 \cdot 10^{21}$   $\mu^+$  decays in the ISIS target. Applying all evaluation cuts, 15 candidate sequences remain with prompt energies as shown in Figure 1. The expected background amounts to  $15.8 \pm 0.5$  events. This number comprises  $3.9 \pm 0.2$  events

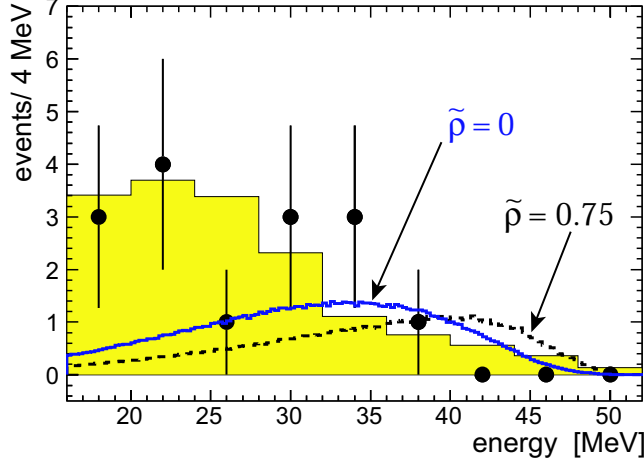


FIG. 1: Visible energy distribution of candidate events with background expectation (shaded area). The solid and dashed lines show the 90% C.L. limit for an additional  $\bar{\nu}_e$  signal with a spectral parameter  $\tilde{\rho} = 0$  and  $\tilde{\rho} = 0.75$ , respectively.

from cosmic induced sequences as well as  $\nu$  induced reactions such as intrinsic source contamination of  $\bar{\nu}_e$  ( $2.0 \pm 0.2$ ),  $\nu_e$  induced random coincidences ( $4.8 \pm 0.3$ ) and  $(e^-, e^+)$  sequences from  $^{12}\text{C}(\nu_e, e^-)^{12}\text{N}_{\text{g.s.}}$  with subsequent  $^{12}\text{N}$  decay ( $5.1 \pm 0.2$ ). Except for the intrinsic  $\bar{\nu}_e$  contamination, which has been deduced from detailed MC simulations, all the background components have been measured in different time and energy regimes with the KARMEN detector and extrapolated into the evaluation cuts applied for this  $\bar{\nu}_e$  search.

## RESULTS AND DISCUSSION

The expected number of  $\bar{\nu}_e$  induced events from  $\mu^+ \rightarrow e^+ + \bar{\nu}_e + (\bar{\nu})$  is determined by the detection efficiencies of the prompt positron and the delayed neutron. The overall detection efficiency for positrons is given in Table I for a set of different spectral parameters  $\tilde{\rho}$  including the contribution from  $^{12}\text{C}(\bar{\nu}_e, e^+ n)^{11}\text{B}$ , which effectively amounts to less than 5% of the  $p(\bar{\nu}_e, e^+)n$  signal in the energy interval of 16–50 MeV.

Based on the Poisson statistics of the numbers of candidate events and expected background, one can extract an energy-independent upper limit for an additional signal [24] of  $N(\bar{\nu}_e) < 7.4$  excess events. However, there is additional spectral information, as can be seen from Figure 1. To use this, we applied a maximum likelihood analysis varying the strength of a  $\bar{\nu}_e$  signal with the energy distribution according to a set of different  $\tilde{\rho}$  parameters. Ta-

TABLE I: Flux averaged cross section  $\langle\sigma\rangle$  for  $p(\bar{\nu}_e, e^+)n$  and  $^{12}\text{C}(\bar{\nu}_e, e^+)^{11}\text{B}$ , total efficiency for  $e^+$  detection, expected  $(e^+, n)$  sequences for  $\mu^+$  decaying entirely via  $\mu^+ \rightarrow e^+ + \bar{\nu}_e + (\bar{\nu})$ , experimental results for potential  $\bar{\nu}_e$ -induced events and deduced upper limits for the branching ratio for different spectral parameters  $\tilde{\rho}$ .

$\tilde{\rho}$	$\langle\sigma\rangle[10^{-42}\text{cm}^2]$		$e^+$ efficiency [16-50] MeV	$N(\bar{\nu}_e)_{\text{BR}=1}$	$N(\bar{\nu}_e)_{\text{bestfit}}$	$N(\bar{\nu}_e)_{90\%\text{CL}}$	BR (90% C.L.)
	$\bar{\nu}_e + p$	$\bar{\nu}_e + ^{12}\text{C}$					
0.0	72.0	4.5	0.450	$4304 \pm 403$	+0.3	$< 7.1$	$< 1.7 \cdot 10^{-3}$
0.25	78.8	5.8	0.452	$4773 \pm 445$	-0.1	$< 6.2$	$< 1.3 \cdot 10^{-3}$
0.5	86.0	7.2	0.456	$5273 \pm 489$	-0.4	$< 6.0$	$< 1.1 \cdot 10^{-3}$
0.75	93.5	8.5	0.462	$5828 \pm 538$	-0.8	$< 5.3$	$< 0.9 \cdot 10^{-3}$

ble I shows the signal strength  $N(\bar{\nu}_e)_{\text{bestfit}}$  from the likelihood method. To extract 90% C.L. intervals for  $N(\bar{\nu}_e)$ , we performed large samples of MC simulations reproducing experiment-like spectra under different signal hypotheses. Our experimental result is consistent with no  $\bar{\nu}_e$  emission from  $\mu^+$  decay with upper limits given in Table I, extracted within a unified frequentist analysis near the physical boundary  $N(\bar{\nu}_e)=0$  following [25].

With a potential signal strength of  $N(\bar{\nu}_e)=5828 \pm 538$  for a branching ratio  $BR=1$  for LF number violating decays and  $\tilde{\rho}(\bar{\nu}_e)=0.75$ , we set an upper limit of the branching ratio of

$$BR = \frac{\Gamma(\mu^+ \rightarrow e^+ + \bar{\nu}_e + (\bar{\nu}); \tilde{\rho}(\bar{\nu}_e)=0.75)}{\Gamma(\mu^+ \rightarrow e^+ + \nu_e + \bar{\nu}_\mu)} < 9 \cdot 10^{-4}$$

with 90% C.L. as well as the upper limits given in Table I for other values of  $\tilde{\rho}(\bar{\nu}_e)$ . Figure 1 shows the visible  $e^+$  energies from  $\mu^+ \rightarrow e^+ + \bar{\nu}_e + (\bar{\nu})$  for two different  $\tilde{\rho}$  parameters with total strength excluded at 90% C.L..

The above limits on the branching ratio  $BR$  on  $\mu^+$  decays emitting  $\bar{\nu}_e$  improve by more than an order of magnitude the most sensitive limit so far of  $BR(\mu^+ \rightarrow e^+ + \bar{\nu}_e + \nu_\mu) < 0.012$  obtained by the E645 experiment at LAMPF [24, 26].

In models extending the SM, the LF violating muon decay  $\mu^+ \rightarrow e^+ + \bar{\nu}_e + \nu_\mu$  is often related to other LF violating processes, e.g.  $\mu \rightarrow 3e$ ,  $\tau \rightarrow \mu ee$  or muonium–antimuonium ( $M\bar{M}$ ) conversion. Therefore, limits such as the limit on the probability for spontaneous conversion  $P(M \rightarrow \bar{M}) < 8.2 \cdot 10^{-11}$  (90% C.L.) [27] set also stringent limits on the coupling

constants responsible for the decay  $\mu^+ \rightarrow e^+ + \bar{\nu}_e + \nu_\mu$  [28? ].

The most conservative upper limit of  $BR < 1.7 \cdot 10^{-3}$  for any parameter  $\tilde{\rho}$  derived here is in direct experimental disagreement with the possibility that the beam excess of  $\bar{\nu}_e$  seen in the LSND experiment with a branching ratio or probability of  $P = (2.64 \pm 0.67 \pm 0.45) \cdot 10^{-3}$  [14] is due to  $\mu^+$  decays with  $\bar{\nu}_e$  emission. In the LSND maximum likelihood analysis of the data, the best fit to the data is found to be an oscillation contribution with the parameters  $\Delta m^2 = 1.2 \text{ eV}^2$  and  $\sin^2(2\Theta) = 0.003$  [14]. In this analysis, oscillation events arise from  $p(\bar{\nu}_e, e^+)n$  with  $\bar{\nu}_e$  via  $\bar{\nu}_\mu \rightarrow \bar{\nu}_e$  from  $\mu^+$  DAR as well as from  $^{12}\text{C}(\nu_e, e^-)^{12}\text{N}$  with  $\nu_e$  via  $\nu_\mu \rightarrow \nu_e$  from  $\pi^+$  decays in flight (DIF). For large  $\Delta m^2$ , about 30 % of the oscillation signal is due to  $\nu_\mu \rightarrow \nu_e$  from DIF, leading to a complex superposition of energy distributions for the prompt events distorted by two different  $L/E$  combinations, with  $L$  being the distance source–detector and  $E$  the neutrino energy.

To be able to compare our result quantitatively with the LSND evidence, we follow the detailed statistical analysis of the LSND data described in [29]. In this analysis, a special cut had been applied to select  $\bar{\nu}_e$  via  $\bar{\nu}_\mu \rightarrow \bar{\nu}_e$  from  $\mu^+$  DAR only with almost no oscillation events from  $\nu_\mu \rightarrow \nu_e$  from  $\pi^+$  DIF. For large differences of the squared mass eigenvalues  $\Delta m^2 = 100 \text{ eV}^2$ , the extracted interval of the mixing amplitude from the parameter region of 90% C.L. was  $3.8 \cdot 10^{-3} < \sin^2(2\Theta) < 8.0 \cdot 10^{-3}$ , with the best fit at  $\sin^2(2\Theta) = 5.8 \cdot 10^{-3}$  corresponding to  $65.8(1.3) \bar{\nu}_e(\nu_e)$  from  $\bar{\nu}_\mu \rightarrow \bar{\nu}_e(\nu_\mu \rightarrow \nu_e)$ , respectively. For such large values of  $\Delta m^2$ , the energy spectrum of  $\bar{\nu}_e$  is in good approximation the one given in equ. (1) with  $\tilde{\rho} = 0.75$  [30]. Assuming 100 % decay probability with a spectral parameter  $\tilde{\rho} = 0.75$ , one would expect 22692  $\bar{\nu}_e$  events seen in the LSND detector. Taking the 65.8  $\bar{\nu}_e$  events deduced by the maximum likelihood analysis as emitted in the decay  $\mu^+ \rightarrow e^+ + \bar{\nu}_e + (\bar{\nu})$ , we extract a branching ratio of  $BR_{\text{LSND}}(\tilde{\rho} = 0.75) = 2.9 \cdot 10^{-3}$  with an approximated 90% C.L. interval of  $1.9 \cdot 10^{-3} < BR_{\text{LSND}} < 4.0 \cdot 10^{-3}$ . Our derived 90% C.L. limit of  $BR < 0.9 \cdot 10^{-3}$  clearly excludes the LSND interval of same confidence and underlines the incompatibility of the two experimental results interpreted in terms of LF violating  $\mu^+$  decays.

We acknowledge financial support from the German Bundesministerium für Bildung und Forschung, the Particle Physics and Astronomy Research Council and the Council for the Central Laboratory of the Research Councils. We thank the Rutherford Appleton Laboratory and the ISIS neutron facility for their hospitality.



- 
- [1] W. Fetscher and H. Gerber, Precision Tests of the Standard Electroweak Model, ed. P. Langacker, World Scientific (1993).
  - [2] B. Armbruster *et al.*, Phys. Rev. Lett. **81**, 520 (1998).
  - [3] P. Langacker and D. London, Phys. Rev. D **39**, 266 (1989).
  - [4] R. Mohapatra and J. Pati, Phys. Rev. D **11**, 566 (1975).
  - [5] P. Herczeg, Zeitschr. Phys. C **56**, 129 (1992).
  - [6] P. Herczeg and R.N. Mohapatra, Phys. Rev. Lett **69**, 2475 (1992).
  - [7] R.N. Mohapatra, Progr. Part. Nucl. Phys. **31**, 39 (1993).
  - [8] H. Fujii *et al.*, Phys. Rev. D **49**, 559 (1994).
  - [9] K.S. Babu and S. Pakvasa, [arXiv:hep-ph/0204236](#).
  - [10] A. Halprin and A. Masiero, Phys. Rev. D **48**, R2987 (1993).
  - [11] B. de Carlos and P.L. White, Phys. Rev. D **54**, 3427 (1996).
  - [12] K.S. Babu *et al.*, [arXiv:hep-ph/0211068](#).
  - [13] G.L. Fogli *et al.*, [arXiv:hep-ph/0212127](#) and references therein.
  - [14] A. Aguilar *et al.*, Phys. Rev. D **64**, 112007 (2001).
  - [15] B. Armbruster *et al.*, Phys. Lett. B **423**, 15 (1998).
  - [16] B. Armbruster *et al.*, Phys. Rev. D **65**, 112001 (2002).
  - [17] B. Armbruster *et al.*, Phys. Rev. C **57**, 3414 (1998).
  - [18] J. Bonn *et al.*, Nucl. Phys. B (Proc. Suppl.) **110**, 395 (2002).
  - [19] C. Bouchiat and L. Michel, Phys. Rev. **106**, 170 (1957).
  - [20] R.L. Burman, A.C. Dodd and P. Plischke, Nucl. Instrum. Methods A **368**, 416 (1996).
  - [21] G. Drexlin *et al.*, Nucl. Instrum. Methods A **289**, 490 (1990).
  - [22] P. Vogel and J.F. Beacom, Phys. Rev. D **60**, 053003 (1999).
  - [23] E. Kolbe, in Proc. of the 5th Int. Symp. on Nuclear Astrophysics, Volos, Greece (1998).
  - [24] K. Hagiwara *et al.*, Phys. Rev. D **66**, 010001 (2002).
  - [25] G.J. Feldman and R.D. Cousins, Phys. Rev. D **57**, 3873 (1998).
  - [26] S.J. Freedman *et al.*, Phys. Rev. D **47**, 811 (1993).
  - [27] L. Willmann *et al.*, Phys. Rev. Lett. **82**, 49 (1999).
  - [28] S. Bergmann and Y. Grossman, Phys. Rev. D **59**, 093005 (1999).

- [29] E.D. Church *et al.*, Phys. Rev. D **66**, 013001 (2002).
- [30] For a quantitative comparison of the results for other values of  $\tilde{\rho}$ , one would need a specific re-analysis of the LSND data.